



CHORUS

This is the accepted manuscript made available via CHORUS. The article has been published as:

Langevin dynamics of correlated subdiffusion and normal diffusion

Yingxi Wang, Nanrong Zhao, and Yijing Yan

Phys. Rev. E **85**, 041142 — Published 26 April 2012

DOI: [10.1103/PhysRevE.85.041142](https://doi.org/10.1103/PhysRevE.85.041142)

The Langevin dynamics of correlated subdiffusion and normal diffusion motion

Yingxi Wang,¹ Nanrong Zhao,^{1,*} and YiJing Yan^{2,3}

¹*College of Chemistry, Sichuan University, Chengdu 610064, China*

²*Department of Chemistry, Hong Kong University of Science and Technology, Kowloon*

³*Hefei National Laboratory for Physical Sciences at the Microscale, University of Science and Technology of China, Hefei, Anhui 230026, China*

We analyze the dissipative dynamics of a particle governed by a two-dimensional generalized Langevin equation with coupled fractional Gaussian noise and white noise in its respective coordinates, assuming the lowest order coupling form. Two situations are studied: in the first the particle is free from external force and in the second the particle is subject to a two-dimensional harmonic potential. We derive the general expressions for the mean values, variances, and velocity autocorrelation function, and evaluate their temporal evolutions via the numerical Laplace inversion technique. Through the analytical results of the short time and long time behaviors, we also explicitly elucidate the effects of fluctuation correlation coupling and inter-oscillator coupling on the dynamic behaviors of the particle. It is shown that in both situations the couplings do not affect the short time behavior of self diffusions in each coordinate, and the subdiffusive and normal diffusive features of these processes resemble those in a one-dimensional system with fractional Gaussian noise and white noise respectively. However, over a long time period, the fluctuation correlation extends the characteristic time scales for the self diffusions of a free particle; while only the inter-oscillator coupling induces a retardation of the relaxation processes of a bounded particle towards equilibrium. Moreover, both couplings generate a cross diffusion, whose long time approximation has two possible forms, the selection of which depends on the relevant time scales of self diffusions in each coordinate.

PACS numbers: 05.40.-a, 02.50.-r, 87.15.Ya, 05.10.Gg

I. INTRODUCTION

Diffusion is one of the fundamental mechanisms for transport of materials in physical, chemical and biological systems [1]. The description of the ubiquitous Brownian motion in Einstein's 1905 work [2] provides one of the cornerstones which underlies the modern approaches to stochastic processes. The coarse-grained normal diffusion assumes an ensemble of noninteracting Brownian particles, resulting in a diffusion equation that involves no memory and is valid only for Markovian processes. Evidently, this normal Brownian motion cannot account for the diffusive processes in many disordered large molecular systems, which exhibit typically non-Markovian characteristics of long-time memory [3]. A major class of anomalous diffusion is subdiffusion. It is a rather general process and has been observed in such as atomic transport in porous substrates [4], cell migration *in vivo* [5], enzymatic binding in crowded cellular environments [6], local viscoelastic response in actin networks [7], and conformational fluctuation of protein molecules [8–11]. One of the mechanisms leading to subdiffusion is the chain dynamics induced distance fluctuations [12] such as Rouse model which has been used extensively in studies of polymers [13]. Subdiffusion has been studied through the ensemble averaged square displacement characteristics of $\langle X^2(t) \rangle \sim t^\alpha$ where $0 < \alpha < 1$, rather than $\alpha = 1$ of normal diffusion. It has also been investigated through

time averaged square displacement using time series $X(t)$ of single particle trajectory. Unlike the normal diffusion, subdiffusion leads in general to the ergodicity breaking [14–19]. The ensemble averaged square displacement and its time averaged counterpart are related but not equal in general.

The present work focuses on the ensemble averaged quantities, with the interest in the processes of a subdiffusion coupled with a normal diffusion motion. The general motivation is to examine the nonequilibrium behavior of two or more Brownian motions that are spatially correlated through their common coupling environment. The multiple dimensionality of Brownian motion is actually rather common in reality. Consider, for example, the electron transfer processes in large molecules. The transfer rate depends on not just the distance between donor and acceptor, but also their relative energy fluctuations, and both of them could be of multiple dimensionality by nature. Most of recent work focused only on the distance fluctuation. For instance, Xie and coworkers [9, 10] adopted a one-dimensional generalized Langevin equation (GLE) model to study the conformational change of a flavin oxidoreductase involved in an electron transfer reaction. The underlying donor-acceptor distance fluctuation is inferred from the observed fluorescence lifetime variation, via the classical electron transfer rate theory [20] with an isotropic superexchange decay parameter. Nonetheless, it was found that some protein-mediated electron transfer processes are sensitive to the protein structure [21]. The resulting electron transfer rate would be given by the multi-pathway model [22] or the approximated atomic packing-density model [23], which is com-

*Electronic address: zhaonanr@scu.edu.cn

posed of through-bond and through-space distinguishable tunneling routes with individual decay parameters. The conformational dynamics would therefore require a multi-dimensional description. Moreover, as mentioned earlier, the description of the underlying electron transfer rate processes should consider also the energy fluctuations. Other examples concern the analysis of complex chemical kinetics in single enzyme molecules [24] and single molecule rupture dynamics [25]. Both the global conformation fluctuation and local energy fluctuation play important roles in determining the physical processes of interest. These fluctuations could be not only both multi-dimensional and also correlated via, for example, their common solvent environment.

The aim of this paper is to provide a basic model analysis relevant to the multi-dimensional diffusive processes. In particular, we examine the ensemble-averaged behavior of correlation between two representing diffusion processes, a subdiffusion coupled with a normal diffusion motion. This is right the sense the two-dimensional Brownian particle is referred to throughout this paper. As a simple generalization, we analyze a two-dimensional GLE given in Sec. II, with a coupled fractional Gaussian noise (FGN) and a white noise (WN) in its respective coordinates. We derive the general expressions of mean values, variances, and velocity autocorrelation function in terms of relaxation functions. Two situations will be studied in Sec. III and Sec. IV: in the first the particle is free from external force, and in the second, the particle is bounded by a two-dimensional coupled harmonic potential. The exact temporal evolutions of the dissipative quantities are obtained numerically, whereas their short time and long time asymptotic behaviors are investigated analytically. The effects of coupling coming from both internal noises and external forces on the dissipative particle dynamics are clarified. Finally we conclude this work in Sec. V.

II. GENERALIZED LANGEVIN EQUATION WITH TWO COUPLED COORDINATES

Consider a Brownian motion with two degrees of freedom, $\mathbf{X}(t) \equiv [X_1(t), X_2(t)]^T$, where the superscript T denotes transposition, described by the following GLE,

$$\ddot{\mathbf{X}}(t) + \frac{\partial U(\mathbf{X})}{\partial \mathbf{X}} + \int_0^t d\tau \mathbf{K}(t-\tau) \dot{\mathbf{X}}(\tau) = \mathbf{F}(t). \quad (1)$$

Here $U(\mathbf{X})$ is an external potential, $\mathbf{K}(t)$ represents a dissipative memory kernel matrix, and $\mathbf{F}(t) \equiv [F_1(t), F_2(t)]^T$ is a random force vector. We assume $F_1(t)$, a FGN closely related to a fractional Brownian motion process [26]. It leads to a subdiffusive process with a broad range of time scales. Its autocorrelation function takes a power-law form,

$$\langle F_1(t)F_1(\tau) \rangle = \eta_\gamma |t-\tau|^{-\gamma}; \quad \text{with } 0 < \gamma < 1, \quad (2)$$

with $\langle \cdot \rangle$ denoting trajectory averaging. The proportionality coefficient η_γ depends on the exponent γ in general

but does not depend on times. Taking into account WN below where WN would amount to $\gamma = 1$ (cf. Eq. (8)), we choose $\eta_\gamma = \eta'(2-\gamma)(1-\gamma)$, also consistent with the conventional treatment of FGN [27]. On the other hand, $F_2(t)$ is treated as a Gaussian WN,

$$\langle F_2(t)F_2(\tau) \rangle = 2\eta\delta(t-\tau), \quad (3)$$

with η being the measure of the white noise strength. It is related to a normal Brownian motion process.

In general, $F_1(t)$ and $F_2(t)$ may correlate with each other. The classical cross-correlation function is $\langle F_1(t)F_2(\tau) \rangle = \langle F_2(t)F_1(\tau) \rangle$. The dissipative memory kernel $\mathbf{K}(t)$ links to the random force $\mathbf{F}(t)$ by the classical fluctuation-dissipation theorem [28],

$$\langle \mathbf{F}(t)\mathbf{F}(\tau)^T \rangle = \beta^{-1}\mathbf{K}(t-\tau), \quad (4)$$

where $\beta \equiv 1/(k_B T)$, with k_B being the Boltzmann constant and T the temperature.

The classical dissipative kernel $\mathbf{K}(t)$ is a real symmetric matrix and satisfies $\mathbf{K}(-t) = \mathbf{K}(t)$. Its diagonal elements are dictated by the autocorrelation functions, Eqs. (2) and (3), resulting in $K_{11}(t) = \beta\eta_\gamma |t|^{-\gamma}$ and $K_{22}(t) = 2\beta\eta\delta(t)$, respectively. The off-diagonal elements $K_{12}(t) = K_{21}(t)$ are cross-correlation functions between two noises. Considering the fact that the spectrum of the memory kernel matrix, $\hat{\mathbf{K}}(\omega) \equiv \int dt e^{i\omega t} \mathbf{K}(t)$, should be positively defined [28, 29], we introduce

$$\tilde{K}_{12}(\omega) = \tilde{K}_{21}(\omega) = \epsilon \sqrt{\tilde{K}_{11}(\omega)\tilde{K}_{22}(\omega)}, \quad (5)$$

with $|\epsilon| \leq 1$ to measure the fluctuation correlation coupling strength between two noises. In general, this coupling could have been different, and ϵ can depend on frequency. However, to elucidate the essential role of noise coupling, we consider its leading term in a Taylor expansion, throughout this work, by treating ϵ rather as a frequency-independent parameter. We obtain

$$K_{12}(t) = \frac{2}{\pi} \beta \epsilon \cos\left[\frac{(1+\gamma)\pi}{4}\right] \Gamma\left(\frac{1+\gamma}{2}\right) \times \sqrt{\eta\eta'\Gamma(3-\gamma)\sin\left(\frac{\gamma\pi}{2}\right)} t^{-(\gamma+1)/2}, \quad (6)$$

where $\Gamma(z)$ is the Gamma function. For later use, we calculate the Laplace transformation of the memory kernel matrix $\mathbf{K}(t)$,

$$\hat{\mathbf{K}}(s) = \begin{bmatrix} k_\gamma s^{\gamma-1} & \epsilon_\gamma \bar{k}_\gamma s^{\frac{\gamma-1}{2}} \\ \epsilon_\gamma \bar{k}_\gamma s^{\frac{\gamma-1}{2}} & k \end{bmatrix}, \quad (7)$$

where

$$k_\gamma \equiv \beta\eta'\Gamma(3-\gamma), \quad k \equiv 2\beta\eta, \quad \bar{k}_\gamma \equiv \sqrt{k_\gamma k/2}, \quad (8)$$

and $\epsilon_\gamma = \frac{2\epsilon}{\pi} \sqrt{\sin(\frac{\gamma\pi}{2})} \cos\left[\frac{(1+\gamma)\pi}{4}\right] \Gamma\left(\frac{1+\gamma}{2}\right) \Gamma\left(\frac{1-\gamma}{2}\right)$, which via the identity $\Gamma\left(\frac{1+\gamma}{2}\right) \Gamma\left(\frac{1-\gamma}{2}\right) = \pi / \sin\left[\frac{(1+\gamma)\pi}{2}\right]$ can be simplified as

$$\epsilon_\gamma = \epsilon \left[\frac{2 \sin(\frac{\gamma\pi}{2})}{1 + \sin(\frac{\gamma\pi}{2})} \right]^{1/2}. \quad (9)$$

It satisfies $0 < \epsilon_\gamma/\epsilon < 1$ for $0 < \gamma < 1$. The larger γ is, i.e., the closer the FGN is to the WN, the larger the value of ϵ_γ/ϵ will be. Apparently, it is the *effective* noise correlation parameter ϵ_γ , rather than ϵ defined in Eq. (5), which plays the role in the GLE (1) and its dynamics as elaborated in the following.

We further consider $U(\mathbf{x})$ is a two-dimensional harmonic potential, characterized by a Hessian matrix \mathbf{w} . The formal solution to the GLE (1) can be obtained by means of the Laplace transformation technique, resulting in

$$\mathbf{X}(t) = \langle \mathbf{X}(t) \rangle + \int_0^t dt' \mathbf{G}(t-t') \mathbf{F}(t'), \quad (10)$$

$$\dot{\mathbf{X}}(t) = \langle \dot{\mathbf{X}}(t) \rangle + \int_0^t dt' \mathbf{g}(t-t') \mathbf{F}(t'), \quad (11)$$

with

$$\langle \mathbf{X}(t) \rangle = [\mathbf{I} - \mathbf{w}\mathbf{Q}(t)]\mathbf{x}_0 + \mathbf{G}(t)\mathbf{v}_0, \quad (12)$$

$$\langle \dot{\mathbf{X}}(t) \rangle = -\mathbf{w}\mathbf{G}(t)\mathbf{x}_0 + \mathbf{g}(t)\mathbf{v}_0. \quad (13)$$

Here, $\mathbf{x}_0 = \mathbf{X}(0)$ and $\mathbf{v}_0 = \dot{\mathbf{X}}(0)$ are the initial values; $\mathbf{G}(t)$ is the dissipative Green function for solving $\mathbf{X}(t)$, given by the Laplace inversion of

$$\hat{\mathbf{G}}(s) = [s^2\mathbf{I} + s\hat{\mathbf{K}}(s) + \mathbf{w}]^{-1}. \quad (14)$$

The integral of $\mathbf{G}(t)$ yields $\mathbf{Q}(t)$:

$$\mathbf{Q}(t) = \int_0^t dt' \mathbf{G}(t'), \quad (15)$$

while the relaxation Green function $\mathbf{g}(t)$ for solving $\dot{\mathbf{X}}(t)$ is

$$\mathbf{g}(t) = \dot{\mathbf{G}}(t). \quad (16)$$

From Eqs. (12) and (13), it follows $\mathbf{G}(0) = 0$ and $\mathbf{g}(0) = \mathbf{I}$. Furthermore, similar to the one-dimensional case [30, 31], it can be shown that the relaxation function $\mathbf{g}(t)$ is identical to the long time behavior of the normalized velocity autocorrelation function (see appendix for the detailed derivation):

$$\mathbf{C}_v(t) = \lim_{\tau \rightarrow \infty} \frac{\langle \dot{\mathbf{X}}(t+\tau)\dot{\mathbf{X}}(\tau)^T \rangle}{\langle \dot{\mathbf{X}}(\tau)\dot{\mathbf{X}}(\tau)^T \rangle} = \mathbf{g}(t). \quad (17)$$

Finally, we obtain the variances as follows:

$$\beta\sigma_{\mathbf{xx}}(t) = 2\mathbf{Q}(t) - \mathbf{G}^2(t) - \mathbf{Q}(t)\mathbf{w}\mathbf{Q}(t), \quad (18a)$$

$$\beta\sigma_{\mathbf{vv}}(t) = \mathbf{I} - \mathbf{g}^2(t) - \mathbf{G}(t)\mathbf{w}\mathbf{G}(t), \quad (18b)$$

$$\beta\sigma_{\mathbf{xv}}(t) = \mathbf{G}(t)[\mathbf{I} - \mathbf{g}(t) - \mathbf{w}\mathbf{Q}(t)]. \quad (18c)$$

All quantities of interest are now expressed in terms of the three relaxation functions, $\mathbf{G}(t)$, $\mathbf{Q}(t)$, and $\mathbf{g}(t)$.

In practice, these three key functions can be evaluated in a streamline manner. For example, one can firstly calculate $\mathbf{Q}(t)$, and then take the first and second time derivatives to obtain $\mathbf{G}(t)$ and $\mathbf{g}(t)$ successively, as suggested by Eqs. (15) and (16). The information about the dissipative particle dynamics is thus followed accordingly by way of means [Eqs. (12) and (13)], velocity autocorrelation function [Eq. (17)], and variances [Eq. (18)]. Note that as $\mathbf{w} \rightarrow 0$, all these quantities of a bounded particle will reduce to those of an unbounded one.

In addition to these exact solutions, we will also analyze the asymptotic behavior of the particle, to elucidate explicitly the effects of fluctuation correlation coupling and inter-oscillator coupling on the dynamics. We will see that a bounded particle is ultimately confined to its equilibrium by a harmonic potential, while a free particle diffuses unboundedly under internal fluctuation. Thus, the long time approximations for unbounded and bounded particles are expected to be quite different. We study these two situations separately in the two coming sections.

III. UNBOUNDED BROWNIAN PARTICLE

For an unbounded Brownian particle, i.e., $\mathbf{w} = 0$, the diffusion process is wholly governed by the frictions induced by its stochastic environment. In addition to the dynamical quantities discussed in the preceding section, the mean square displacement (MSD) $\langle \mathbf{X}(t)\mathbf{X}(t)^T \rangle$, and the relative diffusion coefficient $\mathbf{D}(t)$, will facilitate understanding of the diffusive features of a free Brownian motion. Without loss of generality, it is assumed that $\mathbf{x}_0 = 0$ and the thermal equilibrium condition $\mathbf{v}_0\mathbf{v}_0^T = \beta^{-1}\mathbf{I}$. Using Eqs. (12) and (18a), the mean square displacement can be derived as

$$\langle \mathbf{X}(t)\mathbf{X}(t)^T \rangle = 2\beta^{-1}\mathbf{Q}(t). \quad (19)$$

The diffusion coefficient then, according to the definition [32, 33], follows

$$\mathbf{D}(t) = \frac{1}{2} \frac{d}{dt} \langle \mathbf{X}(t)\mathbf{X}(t)^T \rangle = \beta^{-1}\mathbf{G}(t). \quad (20)$$

Similarly, both MSD and the diffusion coefficient are completely determined by the relaxation functions, i.e., $\mathbf{Q}(t)$ and $\mathbf{G}(t)$, respectively.

To analyze the whole dissipative dynamics, we start with $\mathbf{Q}(t)$. Inserting the memory kernel matrix $\hat{\mathbf{K}}(s)$ of Eq. (7) into Eq. (14), and taking into account that $\hat{\mathbf{Q}}(s) = \hat{\mathbf{G}}(s)/s$, we obtain in Laplace domain,

$$\hat{\mathbf{Q}}(s) = \frac{1}{s^2} \begin{bmatrix} s + k_\gamma s^{\gamma-1} & \epsilon_\gamma \bar{k}_\gamma s^{\frac{\gamma-1}{2}} \\ \epsilon_\gamma \bar{k}_\gamma s^{\frac{\gamma-1}{2}} & s + k \end{bmatrix}^{-1}. \quad (21)$$

Obviously, due to the finite effective cross correlation ($\epsilon_\gamma \neq 0$), the self diffusions in FGN and WN coordinates are entangled with each other, and meanwhile a cross diffusion between these two coordinates arises.

TABLE I: The short time ($t < \tau_s^*$) behaviors of an unbounded particle; see Eq. (23) for the relevant characteristic times τ_1° and τ_2° .

| | FGN | WN |
|--------|----------------------------------------------------|--------------------------------|
| $Q(t)$ | $t^2 E_{2-\gamma,3}[-(t/\tau_1^\circ)^{2-\gamma}]$ | $t^2 E_{1,3}[-t/\tau_2^\circ]$ |
| $G(t)$ | $t E_{2-\gamma,2}[-(t/\tau_1^\circ)^{2-\gamma}]$ | $t E_{1,2}[-t/\tau_2^\circ]$ |
| $g(t)$ | $E_{2-\gamma}[-(t/\tau_1^\circ)^{2-\gamma}]$ | $\exp(-t/\tau_2^\circ)$ |

In what follows, the self diffusion quantities will be denoted with superscripts as ‘FGN’ and ‘WN’ respectively, with the cross quantities as ‘F-W’. In a straightforward manner, the inverse Laplace transformation of Eq. (21) gives the temporal evolution of $\mathbf{Q}(t)$, and then $\mathbf{G}(t)$ and $\mathbf{g}(t)$ are evaluated by its first and second time derivatives. These exact solutions will be obtained with the aid of numerical Laplace transformation technique.

In contrast to the numerically exact results, the approximate solutions in short and long time periods can be obtained with analytical tractability, through which the effect of the fluctuation correlation coupling on the dissipative dynamics can be resolved to a certain degree. Moreover, the normal or abnormal features of the diffusion process could be identified by investigating the long time asymptotic behavior.

We commence with the question of when the fluctuation correlation takes place in action. The off-diagonal terms in Eq. (21) suggest the unbounded correlation time scale would be

$$\tau_s^* = (\bar{k}_\gamma \epsilon_\gamma)^{-\frac{2}{3-\gamma}} = (k_\gamma k \epsilon_\gamma^2)^{-\frac{1}{3-\gamma}}. \quad (22)$$

On the other hand, as inferred from the diagonal terms in Eq. (21), we define the *intrinsic characteristic diffusive times* as

$$\tau_1^\circ = k_\gamma^{-\frac{1}{2-\gamma}} \quad \text{and} \quad \tau_2^\circ = k^{-1}. \quad (23)$$

They measure the relaxation time scales of the two unbounded and uncorrelated coordinates.

When $t < \tau_s^*$, the self diffusions appear as if there is no fluctuation correlation. The resulting short time behaviors of self diffusions in each coordinate are listed in Table I. Here we have used the Laplace inversion formula [34],

$$\mathcal{L}^{-1} \left\{ \frac{s^{a-b}}{s^a - \alpha} \right\} = t^{b-1} E_{a,b}(\alpha t^a), \quad (24)$$

with $E_{a,b}(y)$ being a generalized Mittag-Leffler function [35] defined by a series expansion,

$$E_{a,b}(y) = \sum_{n=0}^{\infty} \frac{y^n}{\Gamma(an+b)}, \quad a, b > 0. \quad (25)$$

Apparently, as depicted in Table I, the key quantities in FGN coordinate depend on both τ_1° and γ , while those in WN coordinate depend on $\tau_2^\circ = k^{-1}$ alone.

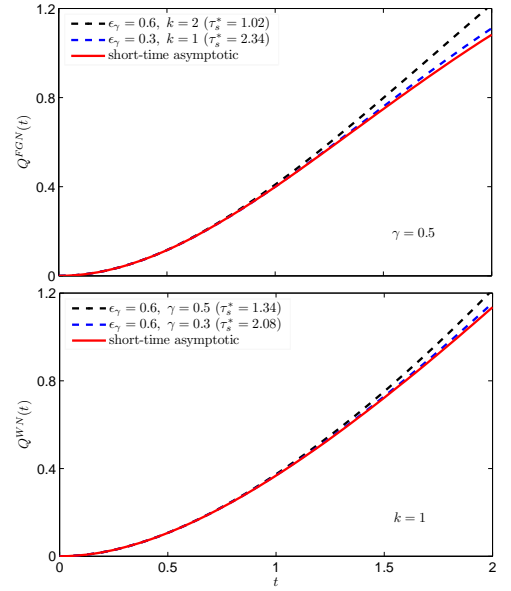


FIG. 1: The self diffusion quantities $Q^{\text{FGN}}(t)$ (upper panel) with $\gamma = 0.5$, and $Q^{\text{WN}}(t)$ (lower panel) with $k = 1$, with $k_\gamma = \Gamma(3-\gamma)$ and an internal unit of $\beta\eta' \equiv 1$ in common. The short time approximations (solid curves) are given in Table I, and depend only on γ and k respectively. The exact results (dash curves) are obtained via the numerical Laplace inversion of Eq. (21), along with other parameters shown in the panels. The corresponding τ_s^* [Eq. (22)] is also specified individually.

Figure 1 depicts the self diffusion quantities $Q^{\text{FGN}}(t)$ and $Q^{\text{WN}}(t)$, with the comparison between the short time approximations (solid curves) given in Table I, and the exact solutions (dash curves) obtained by the numerical Laplace inversion of Eq. (21). We hereafter set $\beta\eta' \equiv 1$ for the internal unit, thus $k_\gamma = \Gamma(3-\gamma)$, as can be seen from Eq. (8). As a result, the short time approximation of FGN is determined by only *one* parameter γ as well. Therefore, we demonstrate $Q^{\text{FGN}}(t)$ with identical γ but different (ϵ_γ, k) , while $Q^{\text{WN}}(t)$ with identical k but different $(\epsilon_\gamma, \gamma)$. It is shown that each type of quantity practically degenerates itself when $t < \tau_s^*$, irrespective of the noise correlation and the fluctuation associated with the counter coordinate. The short time approximations are really excellent when compared with the exact curves in Fig. 1 within τ_s^* .

For the cross diffusion, the short time behavior would better be analyzed with $t < \max\{\tau_1^\circ, \tau_2^\circ\}$. The off-diagonal term in Eq. (21) is found to have one of two possible approximations:

$$Q^{\text{F-W}}(t) \approx \begin{cases} -\epsilon_\gamma \bar{k}_\gamma t^{\frac{1-\gamma}{2}} E_{2-\gamma, \frac{3-\gamma}{2}}[-(t/\tau_1^\circ)^{2-\gamma}], & \tau_1^\circ < \tau_2^\circ \\ -\epsilon_\gamma \bar{k}_\gamma t^{\frac{1-\gamma}{2}} E_{1, \frac{3-\gamma}{2}}(-t/\tau_2^\circ), & \tau_1^\circ > \tau_2^\circ \end{cases}, \quad (26)$$

the selection of which depends on the relative magnitudes of the intrinsic characteristic diffusive times τ_1° and τ_2° .

Figure 2 plots the numerically exact solutions (solid curves) of the cross diffusion $Q^{\text{F-W}}(t)$, versus its short

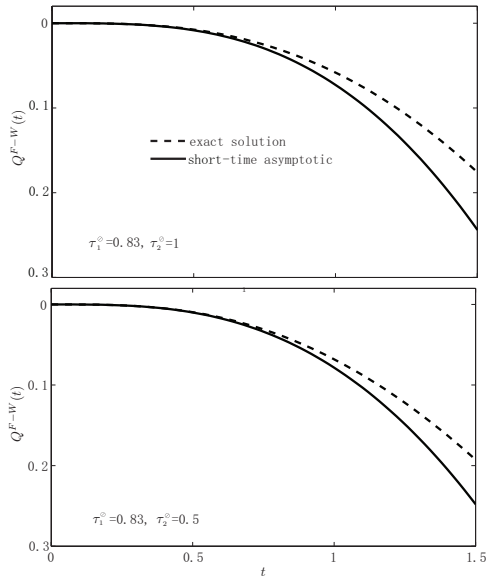


FIG. 2: The cross diffusion quantity $Q^{F-W}(t)$ with $k = 1$ (upper panel) and $k = 2$ (lower panel), with $\gamma = 0.5$ (or $\tau_1^0 = 0.83$), $\epsilon_\gamma = 0.6$, and an internal unit of $\beta\eta' \equiv 1$ in common. The exact solutions (dash curves) are obtained via numerical Laplace inversion of Eq. (21) and the short time approximations (solid curves) are those given by Eq. (26).

time approximations (dash curves) according to Eq. (26), for the two cases of $\tau_1^0 < \tau_2^0$ and $\tau_2^0 < \tau_1^0$, see the values in the figure. The agreement between the exact solutions and approximations is remarkable. It is worth emphasizing here that although the short time behavior of $Q^{F-W}(t)$ [Eq. (26)] is valid when $t < \max\{\tau_1^0, \tau_2^0\}$, it's more accurate when $t < \min\{\tau_1^0, \tau_2^0\}$.

Now we analyze the long time behaviors. From Eq. (21) we have the intermediate expressions

$$\hat{Q}^{\text{FGN}}(s) \approx \frac{s^{-(1+\gamma)}}{s^{2-\gamma} + k_\gamma(1 - \epsilon_\gamma^2)}, \quad (27a)$$

$$\hat{Q}^{\text{WN}}(s) \approx \frac{s^{-2}}{s + k(1 - \epsilon_\gamma^2)}, \quad (27b)$$

$$\hat{Q}^{F-W}(s) \approx -\frac{\epsilon_\gamma \bar{k}_\gamma s^{-\frac{3+\gamma}{2}}}{k s^{2-\gamma} + k_\gamma s + k_\gamma k(1 - \epsilon_\gamma^2)}. \quad (27c)$$

For the self diffusions, Eqs. (27a) and (27b) amount to $Q^{\text{FGN}}(t) = t^2 E_{2-\gamma,3}[-(t/\tau_1)^{2-\gamma}]$ and $Q^{\text{WN}}(t) = t^2 E_{1,3}(-t/\tau_2)$, respectively. The relevant time scales are the *unbounded characteristic times*,

$$\tau_1 \equiv [k_\gamma(1 - \epsilon_\gamma^2)]^{-\frac{1}{2-\gamma}} \quad \text{and} \quad \tau_2 \equiv [k(1 - \epsilon_\gamma^2)]^{-1}. \quad (28)$$

They satisfy $\tau_1 \geq \tau_1^0$ and $\tau_2 \geq \tau_2^0$, with the equal signs holding only when the effective noise correlation ϵ_γ vanishes (i.e., $\epsilon = 0$ or $\gamma \rightarrow 0$ [cf. Eq. (9)]). In other words, the fluctuation correlation leads to a prolonged diffusion time in each coordinate.

TABLE II: The long time asymptotic MSD, diffusion coefficient, and velocity autocorrelation function of an unbounded particle when $t \gg \max\{\tau_1, \tau_2\}$.

| | FGN | WN |
|-------------------------------|-------------------------------------------------------------------------------|---------------------------------------|
| $\beta\langle X^2(t) \rangle$ | $\frac{2}{(1 - \epsilon_\gamma^2)k_\gamma\Gamma(1 + \gamma)}t^\gamma$ | $\frac{2}{(1 - \epsilon_\gamma^2)k}t$ |
| $\beta D(t)$ | $\frac{1}{(1 - \epsilon_\gamma^2)k_\gamma\Gamma(\gamma)}t^{\gamma-1}$ | $\frac{1}{(1 - \epsilon_\gamma^2)k}$ |
| $C_v(t)$ | $-\frac{1-\gamma}{(1 - \epsilon_\gamma^2)k_\gamma\Gamma(\gamma)}t^{\gamma-2}$ | ~ 0 |

With the aid of the asymptotic property of the generalized Mittag-Leffler function [34],

$$E_{a,b}(-y) \approx \frac{1}{y\Gamma(b-a)}, \quad b > a, \quad y > 0, \quad (29)$$

we further obtain the long time behaviors of the key quantities $\mathbf{Q}(t)$, $\mathbf{G}(t)$, and $\mathbf{g}(t)$ when $t \gg \max\{\tau_1, \tau_2\}$. Accordingly, by way of Eqs. (17), (19), and (20), we arrive at the asymptotic solutions of MSD, diffusion coefficient, and velocity autocorrelation function as shown in Table II. In the absence of fluctuation correlation ($\epsilon_\gamma = 0$), these quantities reproduce those obtained in a one-dimensional framework associated with FGN [36] and WN [37].

As evident in Table II, the subdiffusive and normal diffusive features are retained in a two-dimensional correlated system, and resemble those in one-dimensional system with fractional Gaussian noise and white noise respectively. Indeed, in FGN coordinate, MSD takes a form proportional to t^γ , and meanwhile, the diffusion coefficient follows a power-law decay ($\sim t^{\gamma-1}$), tending to zero as $t \rightarrow \infty$. Furthermore, the velocity autocorrelation function exhibits a long *negative* tail. It leads to an incessant change of direction of the velocity and has been named the whip-back effect in literature [38, 39]. The above features characterize a subdiffusive process. On the other hand, in WN coordinate, MSD increases linearly in time, with a finite diffusion coefficient, and the velocity autocorrelation function ($\approx \exp(-t/\tau_2)$) vanishes over a long time period, indicating a normal diffusion. The presence of a fluctuation correlation does not change the self diffusive property, as illustrated above. Nevertheless, it quantitatively strengthens the whip-back effect, enhances the diffusion coefficients, and retards the diffusion processes through prolonging the characteristic time scales [cf. Eq. (28)].

Figure 3 shows the asymptotic solutions (solid curves) of the diffusion coefficient in FGN coordinate, i.e., $D^{\text{FGN}}(t)$, as given in Table II, for several representative values of ϵ_γ . They match well with the numerically exact solutions (dash curves) when $t \gg \max\{\tau_1, \tau_2\}$. Subdiffusive decay with a power-law tail of this quantity is therefore justified. Furthermore, along with the increase of ϵ_γ , the amplitude of $D^{\text{FGN}}(t)$ is augmented, and simultaneously the system takes longer time to approach its equilibrium. It is interesting to note that the peak of this

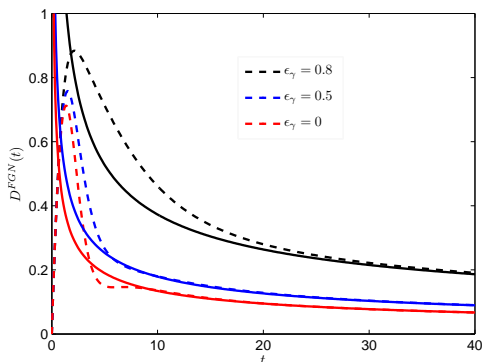


FIG. 3: The long time asymptotic solutions (solid curves) of the diffusion coefficient $D^{\text{FGN}}(t)$ given by Table II. Internal unit of $\beta\eta' \equiv 1$ is used. Three representative curves are obtained with $\gamma = 0.5$ and $k = 1$ in common, and $\epsilon_\gamma = 0$ (red), 0.5 (blue), and 0.8 (black). The corresponding characteristic time sets (τ_1, τ_2) are (0.83, 1), (1, 1.33), and (1.63, 2.78), respectively. The numerically exact results are also presented (dash curves).

quantity is not far from $\max\{\tau_1, \tau_2\}$.

Finally, for cross diffusion when $t \gg \min\{\tau_1, \tau_2\}$, or more appropriately when $t \gg \max\{\tau_1, \tau_2\}$, as will soon be shown, the inverse Laplace transformation of Eq. (27c) firstly leads to two possible intermediate forms as follows:

$$Q^{\text{F-W}}(t) \approx \begin{cases} -\frac{\epsilon_\gamma \bar{k}_\gamma}{k} t^{\frac{5-\gamma}{2}} E_{2-\gamma, \frac{7-\gamma}{2}}[-(t/\tau_1)^{2-\gamma}], & \tau_1 > \tau_2 \\ -\frac{\epsilon_\gamma \bar{k}_\gamma}{k_\gamma} t^{\frac{3+\gamma}{2}} E_{1, \frac{5+\gamma}{2}}(-t/\tau_2), & \tau_2 > \tau_1 \end{cases}, \quad (30)$$

the selection of which depends on the relative magnitudes of the unbounded characteristic times τ_1 and τ_2 . Then, when $t \gg \max\{\tau_1, \tau_2\}$, two possibilities in Eq. (30) reduce to a uniform expression,

$$Q^{\text{F-W}}(t) \approx \frac{\epsilon_\gamma}{\bar{k}_\gamma \Gamma(\frac{3+\gamma}{2})(1-\epsilon_\gamma^2)} t^{\frac{1+\gamma}{2}}. \quad (31)$$

As a result, one obtains immediately

$$\beta \langle X^2(t) \rangle^{\text{F-W}} = \frac{2\epsilon_\gamma}{\bar{k}_\gamma \Gamma(\frac{3+\gamma}{2})(1-\epsilon_\gamma^2)} t^{\frac{1+\gamma}{2}}, \quad (32a)$$

$$\beta D^{\text{F-W}}(t) = \frac{\epsilon_\gamma}{\bar{k}_\gamma \Gamma(\frac{1+\gamma}{2})(1-\epsilon_\gamma^2)} t^{\frac{\gamma-1}{2}}, \quad (32b)$$

$$C_v^{\text{F-W}}(t) = -\frac{\epsilon_\gamma(1-\gamma)}{2\bar{k}_\gamma \Gamma(\frac{1+\gamma}{2})(1-\epsilon_\gamma^2)} t^{\frac{\gamma-3}{2}}, \quad (32c)$$

which feature evidently a subdiffusive cross motion.

IV. PARTICLE BOUNDED BY HARMONIC POTENTIAL

We proceed to consider a two-dimensional Brownian particle confined by a coupled harmonic potential, with

the Hessian matrix,

$$\mathbf{w} = \begin{bmatrix} \omega_1^2 & \lambda\omega_1\omega_2 \\ \lambda\omega_1\omega_2 & \omega_2^2 \end{bmatrix}. \quad (33)$$

Here, ω_1 and ω_2 are the frequencies of oscillators in FGN and WN coordinates, and λ is introduced as a measure of the coupling strength between these two oscillators. With a requirement that \mathbf{w} be positive, we have $|\lambda| < 1$.

Inserting Eqs. (7) and (33) into Eq. (14) leads to

$$\hat{\mathbf{Q}}(s) = \frac{1}{s} \begin{bmatrix} s^2 + k_\gamma s^\gamma + \omega_1^2 & \epsilon_\gamma \bar{k}_\gamma s^{\frac{\gamma+1}{2}} + \lambda\omega_1\omega_2 \\ \epsilon_\gamma \bar{k}_\gamma s^{\frac{\gamma+1}{2}} + \lambda\omega_1\omega_2 & s^2 + k s + \omega_2^2 \end{bmatrix}^{-1}. \quad (34)$$

We proceed to analyze the short time and long time behaviors as follows. First of all, the short time ($t < \min\{1/\omega_1, 1/\omega_2\}$) behavior of the bounded particle is expected to be the same as that of the free particle. Fig. 4 depicts the exact solutions of $Q^{\text{FGN}}(t)$, $Q^{\text{WN}}(t)$ and $Q^{\text{F-W}}(t)$ (dash curves), obtained by the numerical Laplace inversion of Eq. (34). Also included here are the solutions (solid curves) given by Eq. (21) for an unbounded Brownian particle. The figure is obtained with the same noise correlation and fluctuations in each coordinate, but different pairs of oscillatory frequencies. It shows that each type of quantity of a bounded particle degenerates itself and matches well with that of a free particle in a short time period ($t < \min\{1/\omega_1, 1/\omega_2\}$). This justifies the idea that free diffusion provides a good short time approximation for the diffusive process of a harmonically bounded particle.

Next, we turn to the long time analysis. When considering the limit of a long time period, we have

$$\lim_{t \rightarrow \infty} \mathbf{Q}(t) = \lim_{s \rightarrow 0} s \hat{\mathbf{Q}}(s) = \mathbf{w}^{-1}. \quad (35)$$

Therefore, in opposition to the free particle diffusion, the mean square displacement $\langle \mathbf{X}(t) \mathbf{X}(t)^T \rangle = \mathbf{Q}(t) - \mathbf{Q}(t) \mathbf{w} \mathbf{Q}(t)$ will asymptotically tend to zero due to the confining potential. Note that, like Refs. 10 and 40, $U(\mathbf{X})$ is the potential of mean force obtained from $U(\mathbf{X}) = -\beta^{-1} \ln[P(\mathbf{X})]$. $P(\mathbf{X})$ is the two-variable Gaussian probability density function of the stochastic trajectory of $\mathbf{X}(t)$, in the form of $P(\mathbf{X}) \sim \exp(-\frac{1}{2} \beta \mathbf{X}^T \mathbf{w} \mathbf{X})$. $(\beta \mathbf{w})^{-1}$ represents an included equilibrium variance matrix.

For analyzing the long time behaviors before reaching that limit, for simplicity, we omit the off-diagonal term in Eq. (34) arising from fluctuation correlation, i.e., $\epsilon_\gamma \bar{k}_\gamma s^{\frac{\gamma+1}{2}}$, since it will become less and less important compared with the inter-oscillator coupling term $\lambda\omega_1\omega_2$ as time increases. We emphasize here that this simplification is valid only with the premise of finite ω_1 and ω_2 . When ω_1 and ω_2 approach zero, the fluctuation correlation is the only source of coupling. Eq. (34) reduces to the dynamics of an unbounded particle, and the long time approximation follows Eq. (27). In the bounded situation, however, it is the inter-oscillator coupling rather

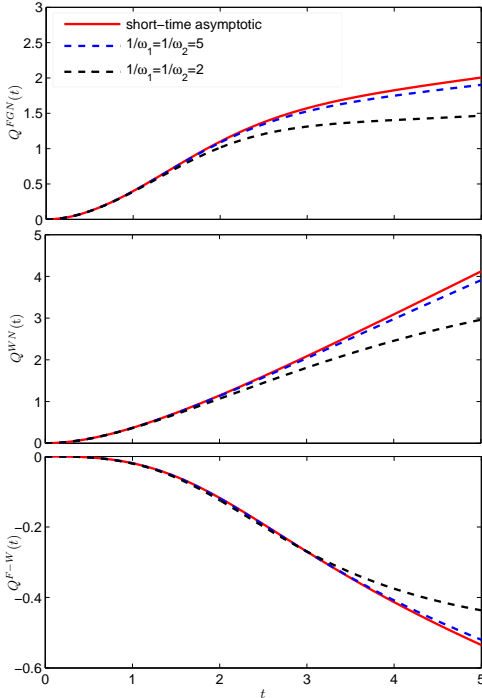


FIG. 4: The self and cross diffusion quantities $Q^{\text{FGN}}(t)$ (upper panel), $Q^{\text{WN}}(t)$ (middle panel), and $Q^{\text{F-W}}(t)$ (lower panel) for a harmonically bounded particle, with common parameters: $\gamma = 0.5$, $k = 1$, $\epsilon_\gamma = 0.2$, and $\lambda = 0.2$, but different values of $\omega_1 = \omega_2 = 0.2$ (blue) and 0.5 (black). Internal unit of $\beta\eta' \equiv 1$ is used. The short time approximations (solid curves) are those given by the free particle diffusion Eq. (21). The exact solutions (dash curves) are obtained via the numerical Laplace inversion of Eq. (34).

than the fluctuation correlation which retains its importance to the coupling effect over a long time period. This leads to a very different asymptotic behavior (see Eq. (36) below). Following similar algebra to Eq. (27), we now obtain

$$\hat{Q}^{\text{FGN}}(s) \approx \frac{1/s}{k_\gamma s^\gamma + \omega_1^2(1-\lambda^2)}, \quad (36a)$$

$$\hat{Q}^{\text{WN}}(s) \approx \frac{1/s}{ks + \omega_2^2(1-\lambda^2)}, \quad (36b)$$

$$\hat{Q}^{\text{F-W}}(s) \approx -\frac{\lambda}{\omega_1\omega_2} \frac{1/s}{\frac{k_\gamma}{\omega_1^2}s^\gamma + \frac{k}{\omega_2^2}s + (1-\lambda^2)}. \quad (36c)$$

As anticipated, the cross term [Eq. (36c)] arises from the λ -mixing rather than the fluctuation correlation [cf. Eq. (27)]. For self diffusions, we obtain from Eqs. (36a) and (36b) the expressions,

$$Q^{\text{FGN}}(t) \approx \frac{1}{\omega_1^2(1-\lambda^2)} [1 - E_\gamma(-t/\bar{\tau}_1)^\gamma], \quad (37a)$$

$$Q^{\text{WN}}(t) \approx \frac{1}{\omega_2^2(1-\lambda^2)} [1 - \exp(-t/\bar{\tau}_2)], \quad (37b)$$

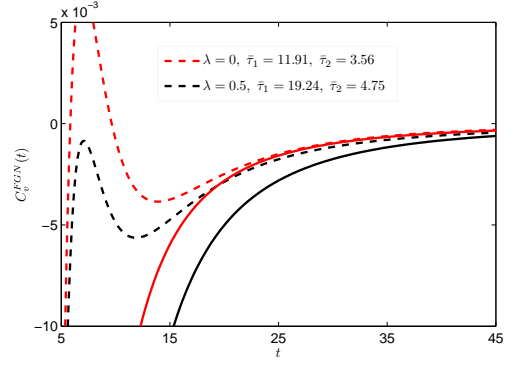


FIG. 5: The numerically exact solutions (dash curves) of velocity autocorrelation function in FGN coordinate, for a harmonically bounded particle, with common parameters: $\gamma = 0.6$, $k = 1$, $\omega_1 = \omega_2 = 0.53$, and $\epsilon_\gamma = 0.2$, but different values of $\lambda = 0$ (red) and 0.5 (black). Internal unit of $\beta\eta' \equiv 1$ is used. The long time asymptotic solutions (solid curves) are given by Eq. (40b).

where

$$\bar{\tau}_1 = \left[\frac{k_\gamma}{\omega_1^2(1-\lambda^2)} \right]^{\frac{1}{\gamma}} \quad \text{and} \quad \bar{\tau}_2 = \frac{k}{\omega_2^2(1-\lambda^2)}. \quad (38)$$

They define the *bounded coupled characteristic times* in FGN and WN coordinates, respectively. For cross diffusion [Eq. (36c)], we further compare the two relevant involved time scales and obtain

$$Q^{\text{F-W}}(t) \approx \begin{cases} \frac{-\lambda\{1 - E_\gamma[(-t/\bar{\tau}_1)^\gamma]\}}{\omega_1\omega_2(1-\lambda^2)}, & \bar{\tau}_1 > \bar{\tau}_2 \\ \frac{-\lambda[1 - \exp(-t/\bar{\tau}_2)]}{\omega_1\omega_2(1-\lambda^2)}, & \bar{\tau}_2 > \bar{\tau}_1 \end{cases}. \quad (39)$$

Obviously, the above $\mathbf{Q}(t)$ [Eqs. (37) and (39)] assumes an equilibrium value in agreement with Eq. (35). Moreover, the inter-oscillator coupling λ extends the time scales of the diffusive processes. This is similar to the role of ϵ_γ played in Eq. (28). The coupling λ also dictates the cross diffusion approaching equilibrium.

The asymptotic behaviors of $\mathbf{G}(t)$ and $\mathbf{g}(t)$ can be obtained via the derivatives of the intermediate expressions of $\mathbf{Q}(t)$ as presented in Eqs. (37) and (39). We will also apply the approximation expression Eq. (29). As a result, over a long time period ($t \gg \bar{\tau}_1$), Eq. (37a) for the FGN coordinate assumes the form

$$G^{\text{FGN}}(t) \approx \frac{k_\gamma \sin(\gamma\pi)}{\pi\omega_1^4(1-\lambda^2)^2} \frac{\Gamma(\gamma+1)}{t^{\gamma+1}}, \quad (40a)$$

$$g^{\text{FGN}}(t) \approx -\frac{k_\gamma \sin(\gamma\pi)}{\pi\omega_1^4(1-\lambda^2)^2} \frac{\Gamma(\gamma+2)}{t^{\gamma+2}}, \quad (40b)$$

while, Eq. (37b) for the WN coordinate assumes the form

$$G^{\text{WN}}(t) \approx \frac{1}{k} \exp(-t/\bar{\tau}_2), \quad (41a)$$

$$g^{\text{WN}}(t) \approx -\frac{\omega_2^2(1-\lambda^2)}{k^2} \exp(-t/\bar{\tau}_2). \quad (41b)$$

Meanwhile, Eq. (39) for the cross diffusion becomes

$$G^{\text{F-W}}(t) \approx \begin{cases} -\frac{\lambda k_\gamma \sin(\gamma\pi)}{\pi\omega_1^3\omega_2(1-\lambda^2)^2} \frac{\Gamma(\gamma+1)}{t^{\gamma+1}}, & \bar{\tau}_1 > \bar{\tau}_2 \\ -\frac{\lambda\omega_2}{\omega_1 k} \exp(-t/\bar{\tau}_2), & \bar{\tau}_2 > \bar{\tau}_1 \end{cases}, \quad (42)$$

$$g^{\text{F-W}}(t) \approx \begin{cases} \frac{\lambda k_\gamma \sin(\gamma\pi)}{\pi\omega_1^3\omega_2(1-\lambda^2)^2} \frac{\Gamma(\gamma+2)}{t^{\gamma+2}}, & \bar{\tau}_1 > \bar{\tau}_2 \\ \frac{\lambda(1-\lambda^2)\omega_2^3}{\omega_1 k^2} \exp(-t/\bar{\tau}_2), & \bar{\tau}_2 > \bar{\tau}_1 \end{cases}. \quad (43)$$

Note that the key quantities of the self diffusion in FGN coordinate are subject to a power-law decay [as seen in Eq. (40)], which features subdiffusive dynamics [31]. Quantities in WN coordinate, in contrast, exhibit an exponential equilibrium rate [as seen in Eq. (41)], characteristic of a normal diffusive process. As $\lambda = 0$, cross diffusion vanishes and the self quantities above reproduce those of a one-dimensional harmonically bounded particle associated with FGN [31] and WN respectively. In the case of WN, the stochastic process is Markovian and its dynamics are well known [41].

Figure 5 presents the exact solutions (dash curves) of the velocity autocorrelation function in FGN coordinate, i.e., $C_v^{\text{FGN}}(t)$, by performing the second derivative of $Q^{\text{FGN}}(t)$. The long time asymptotic solutions (solid curves) are also exhibited according to Eq. (40b), and approximately match the exact ones when $t \gg \bar{\tau}_1$. The subdiffusive decay with a negative power-law tail of this function is well demonstrated. Meanwhile, it is evident that the inter-oscillator coupling λ slows the relaxation towards equilibrium.

Figure 6 shows the exact solutions (dash curves) of the cross velocity autocorrelation function i.e., $C_v^{\text{F-W}}(t)$, versus its long time approximations (solid curves) by using Eq. (43). Two cases of $\bar{\tau}_1 > \bar{\tau}_2$ and $\bar{\tau}_2 > \bar{\tau}_1$ (see the specified values in the figure) are analyzed. It is shown that the coincidence between the approximations and the exact solutions is really excellent when $t > \max\{\bar{\tau}_1, \bar{\tau}_2\}$.

V. CONCLUDING REMARKS

In this work, we analyzed the Langevin dynamics of correlated subdiffusion and normal diffusion motions, assuming a frequency-independent parameter ϵ in Eq. (5), for the fluctuation correlation coupling strength between two noises. The constant ϵ ansatz amounts to the leading contribution in its Taylor expansion, and the resulting correlated Langevin dynamics elucidates the essential role of noise coupling. Two situations are studied: in the first the particle is free from external force and in the second the particle is subject to a two-dimensional harmonic potential. The exact dynamics are derived explicitly, and are evaluated via the numerical Laplace inversion. Furthermore, through the analytical results of the short time and long time behaviors, we elucidate also the effects of

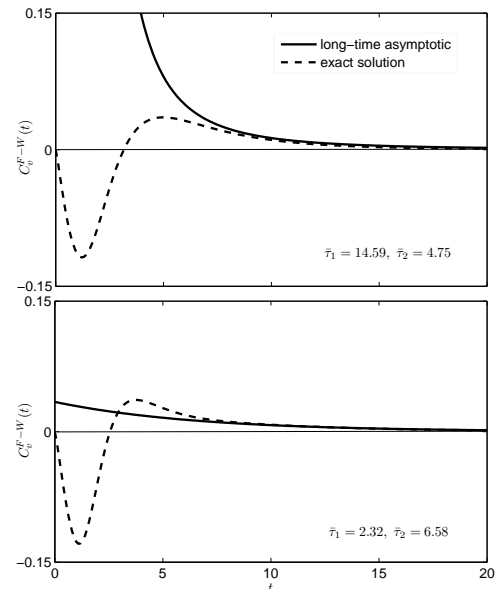


FIG. 6: The numerically exact solutions (dash curves) of velocity autocorrelation function for the cross diffusion of a harmonically bounded particle, with common parameters $k = 1$, $\epsilon_\gamma = 0.2$, and $\lambda = 0.5$, but different other parameter sets ($\gamma = 0.65$, $\omega_1 = \omega_2 = 0.53$) [$\bar{\tau}_1 = 14.59$, $\bar{\tau}_2 = 4.75$] (upper panel), and ($\gamma = 0.6$, $\omega_1 = 1$, $\omega_2 = 0.45$) [$\bar{\tau}_1 = 14.59$, $\bar{\tau}_2 = 4.75$] (lower panel). The long time asymptotic solutions (solid curves) are given by Eq. (43).

fluctuation correlation coupling and inter-oscillator coupling.

As a conclusion, over a short time period, the couplings have no effect on the self diffusions of a particle in each coordinate, in either situation. Meanwhile, the long time analysis shows that the subdiffusive and normal diffusive features of these processes remain when under the effect of coupling and resemble those in one-dimensional system with fractional Gaussian noise and white noise respectively. However, the fluctuation correlation will qualitatively extend the characteristic time scales for the self diffusions of a free particle; while only the inter-oscillator coupling leads to a retardation of the relaxation processes of a bounded particle towards equilibrium. Moreover, both couplings will lead to the presence of a cross diffusion, whose long time approximation has two possible forms. For a free particle, the selection of this approximation depends on the relative magnitudes of the intrinsic characteristic diffusive times; while for a bounded particle, it depends on a comparison of the magnitudes of the bounded coupled characteristic times.

This work can easily be extended to further Langevin dynamics in the framework of multi-dimensional GLE, to describe a variety of phenomena related to concurrent normal and abnormal diffusions. An application of the present theory to the study of the complex chemical kinetics in single enzyme molecules is in progress.

Acknowledgments

Support from National Natural Science Foundation of China (No. 20973119 and No. 21033008) is gratefully acknowledged.

Appendix: Velocity autocorrelation function matrix

This derivation is similar to one done in a one-dimensional GLE [30] framework. We assume that the velocity $\dot{\mathbf{X}}(t)$ relaxes towards a stationary state. In view of $\langle \dot{\mathbf{X}}(t)\dot{\mathbf{X}}(t)^T \rangle \rightarrow \beta^{-1}\mathbf{I}$ as $t \rightarrow \infty$, the normalized velocity autocorrelation function is expressed by

$$\begin{aligned} \mathbf{C}_v(\tau) &= \lim_{t \rightarrow \infty} \frac{\langle \dot{\mathbf{X}}(t+\tau)\dot{\mathbf{X}}(t)^T \rangle}{\langle \dot{\mathbf{X}}(t)\dot{\mathbf{X}}(t)^T \rangle} \\ &= \beta \lim_{t \rightarrow \infty} \langle \dot{\mathbf{X}}(t+\tau)\dot{\mathbf{X}}(t)^T \rangle. \end{aligned} \quad (\text{A.1})$$

By inserting Eq. (11) into the above expression and using the fluctuation-dissipation theorem (4), we have

$$\mathbf{C}_v(\tau) = \beta \lim_{t \rightarrow \infty} \int_0^{t+\tau} dt_1 \int_0^t dt_2 \mathbf{g}(t_1)\mathbf{K}(t_2 + \tau - t_1)\mathbf{g}^T(t_2).$$

Its Fourier transformation can be proven to be real, by

$$\tilde{\mathbf{C}}_v(\omega) = 2\beta \text{Re}[\mathbf{M}(i\omega)], \quad (\text{A.2})$$

where

$$\begin{aligned} \mathbf{M}(i\omega) &= \int_0^\infty d\tau e^{-i\omega\tau} \int_0^t dt_2 \mathbf{g}(t_2) \int_0^t dt_1 \mathbf{K}(t_2 + \tau - t_1) \mathbf{g}^T(t_1) \\ &= \int_0^\infty dt_2 e^{i\omega t_2} \mathbf{g}(t_2) \int_0^\infty d\tau e^{-i\omega(\tau+t_2-t_1)} \\ &\quad \times \mathbf{K}(\tau - t_1 + t_2) \int_0^\infty dt_1 e^{-i\omega t_1} \mathbf{g}(t_1) \\ &= \hat{\mathbf{g}}^*(i\omega)\hat{\mathbf{K}}(i\omega)\hat{\mathbf{g}}(i\omega), \end{aligned} \quad (\text{A.3})$$

with $\hat{\mathbf{g}}(i\omega)$ and $\hat{\mathbf{K}}(i\omega)$ representing the Laplace transformation of $\mathbf{g}(\tau)$ and $\mathbf{K}(\tau)$, evaluated at $s = i\omega$. $\hat{\mathbf{g}}^*(i\omega)$ is the conjugate of $\hat{\mathbf{g}}(i\omega)$. According to Eq. (16), $\hat{\mathbf{g}}(i\omega) = i\omega\hat{\mathbf{G}}(i\omega)$. By taking into account Eq. (14) and the fact that $\hat{\mathbf{K}}(i\omega)$ and \mathbf{w} are symmetric matrixes, we obtain

$$\tilde{\mathbf{C}}_v(\omega) = \beta [\hat{\mathbf{g}}(i\omega) + \hat{\mathbf{g}}^*(i\omega)]. \quad (\text{A.4})$$

Its inverse Fourier transformation finally yields

$$\mathbf{C}_v(\tau) = \beta \int_{-\infty}^\infty d\omega e^{i\omega\tau} \tilde{\mathbf{C}}_v(\omega) = \beta \mathbf{g}(\tau). \quad (\text{A.5})$$

This is just Eq. (17).

-
- [1] P. Hanggi and F. Marchesoni, *Chaos* **15**, 026101 (2005).
[2] A. Einstein, *Investigations on the Theory of Brownian Movement*, Dover, New York, 1956.
[3] J. P. Bouchaud and A. Georges, *Phys. Rep.* **195**, 127 (1990).
[4] P. Brault, C. Josserand, J. M. Bauchire, A. Caillard, C. Charles, and R. W. Boswell, *Phys. Rev. Lett.* **102**, 045901 (2009).
[5] P. Dietrich, R. Klages, R. Preuss, and A. Schwab, *Proc. Natl. Acad. Sci. U.S.A.* **105**, 459 (2008).
[6] S. B. Yuste and K. Lindenberg, *Phys. Rev. E* **76**, 051114 (2007).
[7] F. Amblard, A. C. Maggs, B. Yurke, A. N. Pargellis, and S. Leibler, *Phys. Rev. Lett.* **77** 4470 (1996).
[8] H. Yang, G. Luo, P. Karnchanaphanurach, T. M. Louie, I. Rech, S. Cova, L. Xun, and X. S. Xie, *Science* **302**, 262 (2003).
[9] S. C. Kou and X. S. Xie, *Phys. Rev. Lett.* **93**, 180603 (2004).
[10] W. Min, G. Luo, B. J. Cherayil, S. C. Kou, and X. S. Xie, *Phys. Rev. Lett.* **94**, 198302 (2005).
[11] R. Granek and J. Klafter, *Phys. Rev. Lett.* **95**, 098106 (2005).
[12] J. Tang and R. A. Marcus, *Phys. Rev. E* **73**, 022102 (2006).
[13] M. Doi and S. F. Edwards, *The Theory of Polymer Dynamics*, Clarendon Press, Oxford, 1986.
[14] J. P. Bouchaud, *J. Phys. I France* **2**, 1705 (1992).
[15] G. Bel and E. Barkai, *Phys. Rev. Lett.* **94**, 240602 (2005).
[16] I. Golding and E. C. Cox, *Phys. Rev. Lett.* **96**, 098102 (2006).
[17] I. M. Tolic-Norrelykke, E.-L. Munteanu, G. Thon, L. Oddershede, and K. Berg-Sørensen, *Phys. Rev. Lett* **93**, 078102 (2004).
[18] Y. He, S. Burov, R. Metzler, and E. Barkai, *Phys. Rev. Lett* **101**, 058101 (2008).
[19] J.-H. Jeon, V. Tejedor, S. Burov, E. Barkai, C. Selhuber-Unkel, K. Berg-Sørensen, L. Oddershede, and R. Metzler *Phys. Rev. Lett* **106**, 048103 (2011).
[20] J. J. Hopfield, *Proc. Natl. Acad. Sci. U. S. A.* **71**, 3640 (1974).
[21] T. R. Prytkova, I. V. Kurnikov, and D. N. Beratan, *Science* **315**, 622 (2007).
[22] D. N. Beratan, J. N. Betts, and J. N. Onuchic, *Science* **252**, 1285 (1991).
[23] M. L. Jones, I. V. Kurnikov, and D. N. Beratan, *J. Phys. Chem. A* **106**, 2002 (2002).
[24] S. Chaudhury and B. J. Cherayil, *J. Chem. Phys.* **125**, 024904 (2006).
[25] O. K. Dudko, G. Hummer, and A. Szabo, *Phys. Rev. Lett* **96**, 108101 (2006).
[26] B. B. Mandelbrot and J. van Ness, *SIAM Rev.* **10**, 422 (1968).
[27] H. Qian, *Lecture Notes in Physics* **621**, 22 (2003).
[28] R. Kubo, *Rep. Prog. Phys.* **29**, 255 (1966).
[29] A. A. Budini and M. O. Caceres, *Phys. A* **356**, 31 (2005).

- [30] J. M. Porra, K. G. Wang, and J. Masoliver, Phys. Rev. E **53**, 5872 (1996).
- [31] A. D. Viñales and M. A. Desposito, Phys. Rev. E **73**, 016111 (2006).
- [32] N. Pottier, Physica. A **317**, 371 (2003).
- [33] R. Morgado, F. A. Oliveira, G. G. Batrouni, and A. Hansen, Phys. Rev. Lett. **89**, 100601 (2002).
- [34] I. Podlubny, *Fractional Differential Equations*, Academic Press, London, 1999.
- [35] H. Bateman and A. Erdelyi, *Higher Transcendental Functions*, Robert E. Krieger, Malabar, Florida, 1981.
- [36] R. Kupferman, J. Stat. Phys. **114**, 291 (2004).
- [37] R. Zwanzig, *Nonequilibrium Statistical Mechanics*, Oxford University Press, New York, 2001.
- [38] R. Muralidhar, D. Ramkrishna, H. Nakanishi, and D. Jacobs, Physica A **167**, 539 (1990).
- [39] E. Lutz, Europhys. Lett. **54**, 293 (2001).
- [40] W. Min, B. P. English, G. Luo, B. J. Cherayil, S. C. Kou, and X. S. Xie, Acc. Chem. Res. **38**, 923 (2005).
- [41] H. Risken, *The Fokker Planck Equation*, Springer, Berlin, 1996.